

COMPUTATIONAL DESIGN OF A COMPOSITE RACE CAR SEAT MEETING INTERNATIONAL REGULATION STANDARDS

Johann Sienz^a, Mariela Luege^b and Fabian Fuerle^a

^a*Civil and Computational Engineering Centre, Swansea University, Swansea, UK,
J.Sienz@swansea.ac.uk, <http://www.swan.ac.uk>*

^b*Universidad Nacional de Tucumán, San Miguel de Tucumán, Argentina*

Keywords: Composite racing car seat, simulation based product design.

Abstract. International regulations on the design of racing cars place safety at the top list of the vehicle and vehicle parts design requirements. Numerical simulations is an essential tool for the optimal design of such safety critical car components. The aim of this work is to find the minimal thickness of a fibre reinforced composite structure that can be used in a race car seat subjected to homologation testing. Simulation based product design is used to find a design that passes the three prescribed homologation standards. A finite element model is developed that includes (i) the modelling of the contact between the seat and the loading pads, (ii) the modelling of the bonding between the different parts of the seat, and (iii) the modelling of the effective properties of the composite using the mixture rule. Since the new standards on racing seats prescribe quasi-static tests to ensure controlled load application conditions, a nonlinear-quasi static analysis is performed. Details on the optimal design of the structure, state of deformation and stress of the optimal design are finally given and discussed.

1 INTRODUCTION

For the given geometry for a composite racing car seat as shown in Figure 1, the objective is to identify a minimum value for the car seat thickness and weight in order to pass the homologation tests: FIA standard 8862-2009 (FIA 2010) for advanced racing seats and/or FIA Standard 8855-1999 for competition seats (FIA 2003). Standard 8862 (FIA 2010) requires three quasi-static tests as it is shown in Figure 2: one side, one rear and a crush loading on the seat side shoulders. Standard 8855 instead requires three impact tests, two on the rear and one on the side of the car seat.

The seat is composed of two parts; the seat itself and a lower shell. These two parts are bonded together with AV4076 epoxy resin. The composite structure of the seat is made of one layer of carbon fibre woven fabric (2x2 Twill, 200 g/m², approx. 0.2mm thickness) and either layers of triaxial glass fibre fabric (stacking sequence: 0/-45/+45, 917 g/m², approx. 0.88mm thickness) or layers of bi-diagonal carbon fibre fabric (stacking sequence: -45/+45, 411 g/m², approx. 0.56mm thickness). Infusion resin Norsodyne E9159 (unsaturated polyester) is employed for the injection process. The lower shell is made of only triaxial glass fibre layers.



Figure 1: Geometry of the upper (red) and lower (green) parts of the car seat.

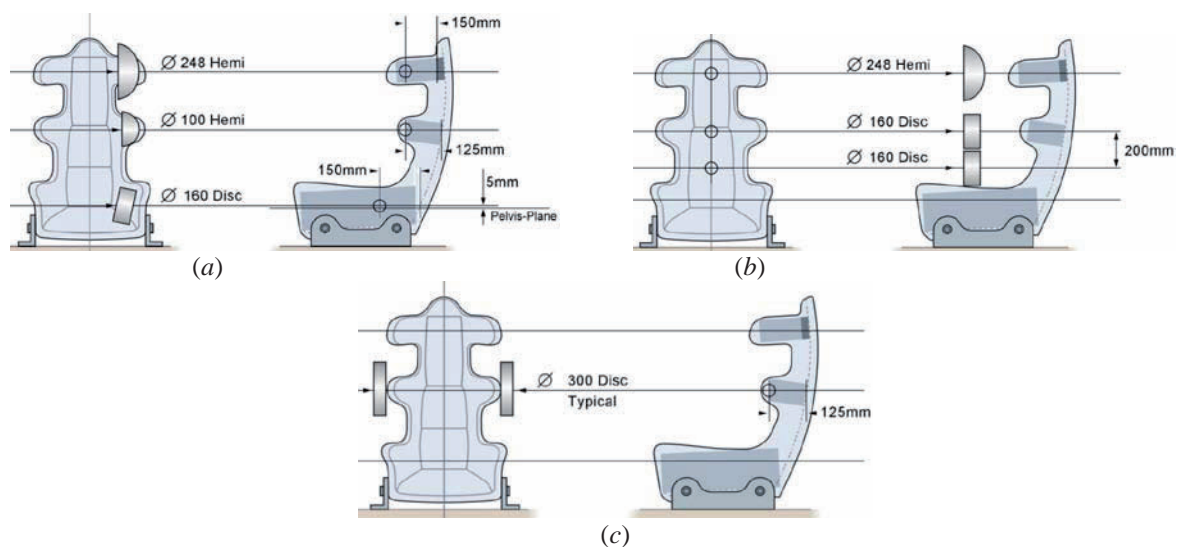


Figure 2: Quasi-static tests for advanced racing car seats: Standard 8862. Side test (a); Rear test (b); Crush test (c).

The main objective is to find the minimum number of glass or carbon fibre layers necessary to pass the homologation tests.

The current design of the seat has been investigated subjected to Standard 8862: Rear and Side loading tests (see Figure 2). Using computer simulation techniques based on the finite element (FE) method, nonlinear analyses with contact simulations have been carried out using the FE optimization software Altair Hyperworks, Release 10.0 (Altair 2010).

The numerical simulations indicate that, by using triaxial glass fibre layers, a minimum seat thickness of 6.38mm (corresponding to a weight of 7.405kg) is required to obtain displacements below the maximum allowable. Nevertheless, concentration of high stresses can be observed where the back middle and shoulder loading pads are applied, along the seat edges and surrounding the belt slots. The stress levels lead to the failure according to the Tsai-Hill failure criterion. Moreover, the first layer of carbon fibre woven fabric appears completely damaged, while the following glass fibre layers show localized failure areas. The lower shell, with a thickness of 6.16mm (for a weight equal to 4.270kg) shows high stress localized at the attachment points.

When using bidiagonal carbon fibre layers, instead of glass fibre layers, a minimum seat thickness of 4.7mm (corresponding to a weight of 4.468kg) is required to obtain displacements below the maximum allowable. As in the previous case, concentration of high stresses can be observed where the back middle and shoulder loading pads are applied, along the seat edges and surrounding the belt slots. In this case, the Tsai-Hill failure criterion is violated in localized areas. The thickness of the lower shell in this case is 4.4mm (for a weight equal to 3.05kg) with high stresses localized at the attachment points.

The following sections contain the details of the problem formulation and the results.

2 SEAT MODEL

In this section the FE model considered in the numerical simulations is shortly described. It consists of the description of the type of FEs used, the material lay-up, material properties, loading and constraint conditions.

2.1 FE Mesh

The FE mesh for the geometrical model shown in Figure 1 has been realized using 94929 shell FEs (92702 quadrilateral and 2227 triangles).

2.2 Material Lay-Up

Based on discussions with suppliers and manufacturers, the following material lay-ups have been assumed in the simulations:

Design 1

Seat (Weight= 7.405kg, thickness=6.38mm):

1 x carbon fibre/resin (2X2 twill fabric)

7 x tri-axial glass/resin (0/-45/+45)

Seat lower shell (Weight= 4.270kg, 6.16mm):

7 x tri-axial glass/resin (0/-45/+45)

Design 2

Seat (Weight= 5.350kg, thickness=4.62mm):

1 x carbon fibre/resin (2X2 twill fabric)

5 x tri-axial glass/resin (0/-45/+45)

Seat lower shell (Weight= 3.050kg, thickness=4.4mm):

5 x tri-axial glass/resin (0/-45/+45)

Design 3

Seat (Weight= 7.192kg, thickness=6.16mm):

7 x tri-axial glass/resin (0/-45/+45)

Seat lower shell (Weight= 4.270kg, thickness=6.16mm):

7 x tri-axial glass/resin (0/-45/+45)

Design 4

Seat (Weight= 4.468kg, thickness=4.7mm):

1 x carbon fibre/resin (2X2 twill fabric)

8 x bidiagonal carbon/resin (-45/+45)

Seat lower shell (Weight= 3.050kg, thickness=4.4mm):

5 x tri-axial glass/resin (0/-45/+45)

2.3 Material Properties

Following discussions with the customer and the manufacturer it was decided to use SAERTEX fabrics (SAERTEX 2010) to build the composite structure of the seat. Those fabrics are also known as Non-Crimp Fabrics (NCF, SAERTEX 2010), and are distinguished by their stretched fibres inside the individual layers as is shown in Figure 3. NCF optimally absorb mechanical forces, such as pressure and tension, and are available as unidirectional, bidirectional and multi-axial stitch bonded constructions.

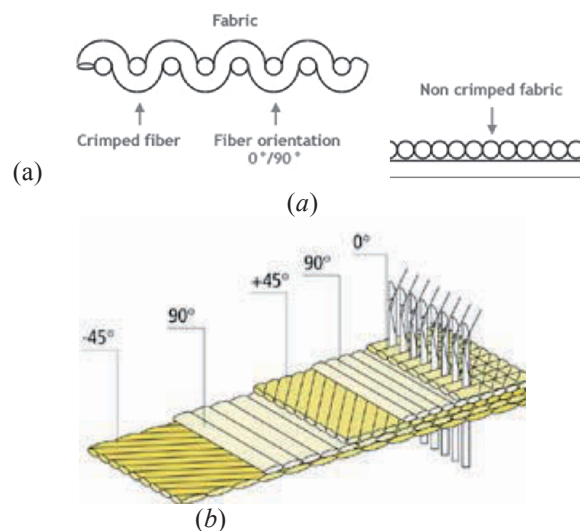


Figure 3. Comparison between Crimped and Non Crimp Fabrics (a); arbitrary fibre orientation of a Non Crimp Fabrics(b) (SAERTEX 2010)

The seat's composite structure is constructed using layers of carbon fibre woven fabric, and either tri-axial glass fibre fabrics or bi-diagonal carbon fibre fabrics, injected with the appropriate infusion resin. The use of Altair Hyperworks (ALTAIR 2010) as FE software requires the properties of each final fibre/resin layer to be introduced independently. Assuming a fibre volume fraction for each composite layer of $V_f=0.4$, Table 1 summarizes the calculated properties for each type of layer, where: E , E_1 , and E_2 are the isotropic, longitudinal and transverse elastic modulus, respectively; G and G_{12} are the Shear Modulus; ν is the

Poisson ratio; $\sigma_{1(2)T(C)}^u$ is the ultimate traction (compression) strength in the longitudinal (transverse) direction; τ^u is the in-plane shear strength and ρ is the density of the material. The interlaminar allowable shear strength, S^u , is assumed equal to 80MPa.

Uni-axial Glass/Resin $V_f=0.4$	Uni-axial Carbon/Resin $V_f=0.4$	Woven Carbon/Resin $V_f=0.4$	Interlaminar strength
$E_1=53000$ MPa	$E_1=92857$ MPa	$E=61800$ MPa	$S^u=80$ MPa
$E_2=12000$ MPa	$E_2=5295$ MPa	$G=3710$ MPa	
$G_{12}=4200$ MPa	$G_{12}=3102$ MPa		
$\nu=0.3$	$\nu=0.3$	$\nu=0.037$	
$\sigma_{1T}^u=880$ MPa	$\sigma_{1T}^u=1024$ MPa	$\sigma_{1T}^u=587$ MPa	
$\sigma_{1C}^u=400$ MPa	$\sigma_{1C}^u=702.9$ MPa	$\sigma_{1C}^u=454$ MPa	
$\sigma_{2T}^u=23$ MPa	$\sigma_{2T}^u=24$ MPa		
$\sigma_{2C}^u=94$ MPa	$\sigma_{2C}^u=79.4$ MPa		
$\tau^u=80$ MPa	$\tau^u=71.9$ MPa	$\tau^u=62.4$ MPa	
$\rho=0.00176$ g/mm ³	$\rho=0.001432$ g/mm ³	$\rho=0.00146$ g/mm ³	

Table 1. Material properties adopted for the unidirectional glass fibre/resin, uniaxial carbon fibre/resin and woven carbon fibre/resin layers.

Since tri-axial glass layers and bi-diagonal carbon layers are constructed using unidirectional fibre plies (as is shown in Figure 3 (b)), the material properties are introduced considering the following: each tri-axial glass fibre/resin layer is simulated as three independent uni-directional glass fibre plies orientated at 0, -45 and 45 degrees, with thicknesses of 0.41mm, 0.235mm and 0.235mm, respectively. Each bi-diagonal carbon fibre/resin layer, instead, is simulated as two independent uni-directional glass fibre plies orientated at -45 and 45 degrees, with thicknesses of 0.28mm, respectively.

2.4 Loading and Constraint Conditions

Loading and constraint conditions are shown in Table 2 and Table 3 for the rear and side loading tests, respectively. The maximum deflection required for the homologation tests are also shown. Loading pads have been simulated using rigid surfaces, which are shown in grey colour. Fully clamped constraint conditions are applied to the lower shell part of the seat. These are highlighted in yellow. The lower and upper part of the seat are 'perfectly bonded' together by using 18389 rigid elements. To search for the contact between seat and loading pads, contact elements have been introduced.

3 CASE STUDIES

Using the FE software Altair Hyperworks 10.0, a nonlinear quasi-static analysis has been performed for the two loading conditions: rear loading and side loading. The response of the material constituents, i.e. the carbon fibre, the glass fibre and the resin, has been assumed to be linear elastic. Since epoxy (polyester) resin can have deformations of more than 400% before breaking, it has been assumed that glass and carbon fibres fail before the resin does. No

plastic deformation can be expected in the composite laminate due to the brittle nature of carbon and glass fibre behaviour. Failure index values corresponding to the Tsai-Hill anisotropic criterion and the interlaminar bonding criterion are then computed using the strength ultimate values given in Table 1.

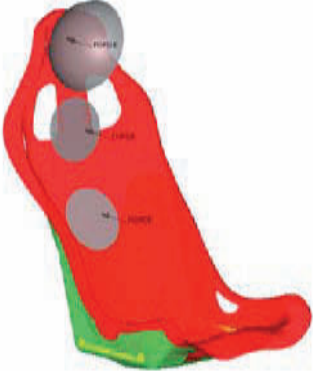
	<p>Applied Loads:</p> <p>Seat Back head: 7 kN</p> <p>Seat back shoulder: 14 kN</p> <p>Seat back middle: 14 kN</p> <p>Constraints(attachments) in yellow: Fully clamped</p>	<p>Maximum deflection</p> <p>120 mm</p> <p>100 mm</p> <p>80 mm</p>
---	---	---

Table 2. Rear loading test: Constraints, loading conditions and maximum deflection.


	<p>Applied Load:</p> <p>Seat side load: 14 kN</p> <p>Constraints in yellow: Fully clamped</p>	<p>Maximum deflection (side direction)</p> <p>40 mm</p>
---	--	--

Table 3. Side loading test: Constraints, loading conditions and maximum deflection.

3.1 Rear loading test

The numerical results, obtained by solving the rear loading test of Table 2, are depicted in Figure 4 to Figure 13. Figure 4 and Figure 5 display the resulting displacement distribution in the rear direction. For Design 1, displacements on the Seat Back Head, Shoulder and Middle are around 111.0mm, 55.0 mm, and 23mm, respectively, low enough compared with the allowed maximum deflections of 120mm, 100mm and 80mm, respectively. For Design 2, the displacements at the same positions are around 174.0mm, 99.0mm, and 25mm, which are greater than the allowed values for the maximum deflections. For Design 3, the displacements are respectively around 130.0mm, 74.0mm, and 18.0mm, again greater than the allowed values for the maximum deflections. For Design 4, the displacements at the same positions are 103.0mm, 50.0mm, and 21.0mm, lower than the maximum allowed values. The distribution of the maximum principal stress is displayed in Figure 6 to Figure 9, showing in all cases high values where the back middle load pad is applied, on the shoulder edges and holes, on the belt's slots and at the attachment points of the lower shell. Higher values of stresses are

observed for Design 2 and Design 4, than for Design 1 and Design 3. It is important to notice that the high stress values obtained with the Design 4 are due to the higher stiffness of the carbon fibre with respect to the glass fibre. Failure index values corresponding to the Tsai-Hill anisotropic criterion are shown in Figure 10 to Figure 13 for Design 1 to Design 4, respectively, where index values above 1.0 denote violation of the Tsai-Hill criterion. From these values, it can therefore be expected that the material will be highly damaged, although Design 3, i.e. a glass fibre seat, and Design 4, i.e. the carbon fibre seat, seem to show better performance. Here, it is worth observing that, since Design 3 shows only localized damage behaviour we can deduce that Design 1's main problem is the woven carbon layer, which completely fails, and not the glass fibre layers, which seem to cope quite well with the loading. Nevertheless, the weight of the glass fibre seat seems to be higher than the requirements.

3.2 Side Loading Test

Constraints and loading conditions for the side loading test are reported in Table 3. The results of the finite element simulation are displayed in Figure 14 to Figure 23. The displacement distribution for Designs 1, 2, 3 and 4 are depicted in Figure 14 and Figure 15, with maximum values of 2.327mm , 3.307mm , 2.5mm and 2.458mm , respectively. These values are lower than the maximum allowable value (40mm). Figure 16 to Figure 19 show the correspondent distribution of the maximum principal stresses, whereas failure index of the Tsai-Hill criterion are depicted in Figure 20 and Figure 23. It is observed that high values of stress and failure index (greater the one) are found around the loading pad.

An overview of the numerical results is shown in Table 4.

Design:	1	2	3	4
Weight (kg) seat/lower shell	7.405/4.27	5.35/3.05	7.192/ 4.27	4.47/3.05
Test 1				
Deflection (mm) (allow. 40)	2.33	3.31	2.50	2.46
Max. Ppal Stress (MPa)	452	905	625	1199
Failure	Carbon: localized Glass: localized	Carbon: localized Glass: localized	Carbon: n.a. Glass: localized	Carbon: localized Glass: localized
Test 2				
Deflection (mm) head/shoulder/back (allow. 20/100/80)	111/55/23	174/ 99/ 25	130/74/18	103/50/21
Max. Ppal Stress (MPa)	579	1025	600	1199
Failure	Carbon: global Glass: localized	Carbon: global Glass: localized	Carbon: n.a. Glass: localized	Carbon: localized Glass: localized

Table 4: Tests 1 and 2: Overview of the numerical results obtained for Designs 1 to 4.

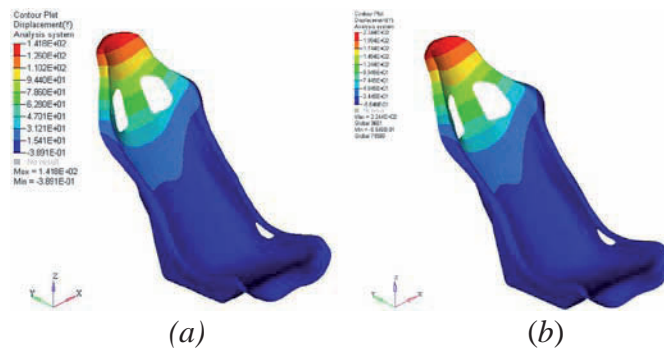


Figure 4: Displacements in the direction y (rear) for: (a) Design 1 (one carbon woven fabric + woven seven tri-axial glass fibre layers) and (b) Design 2 (one carbon woven fabric + five tri-axial glass fibre layers).

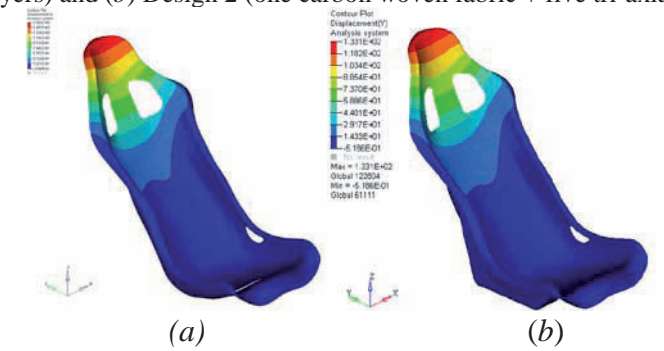


Figure 5: Displacements in the direction y (rear) for: (a) Design 3 (seven tri-axial glass fibre layers) and (b) Design 4 (one carbon woven fabric + eight bidiagonal carbon fibre layers).

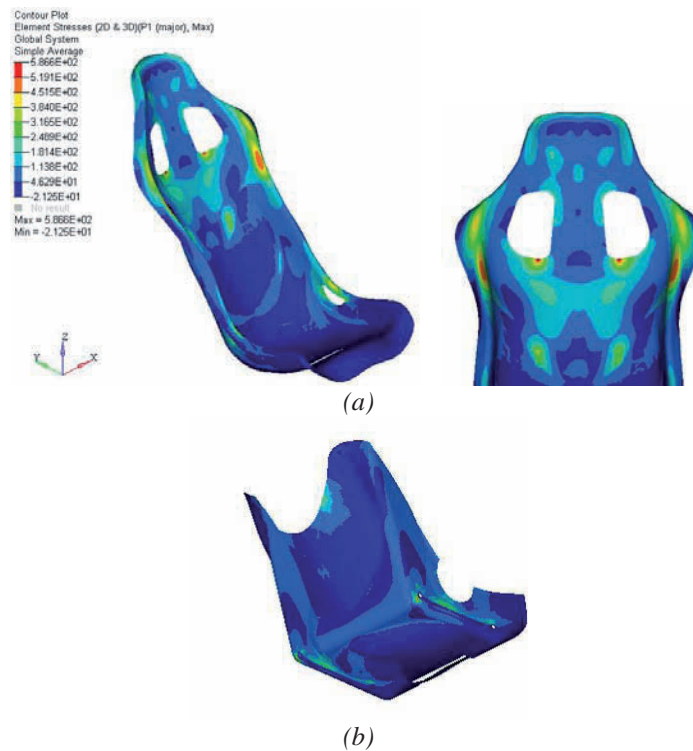


Figure 6. Design 1: Maximum principal stress distribution (a) of the seat and (b) of the lower shell.

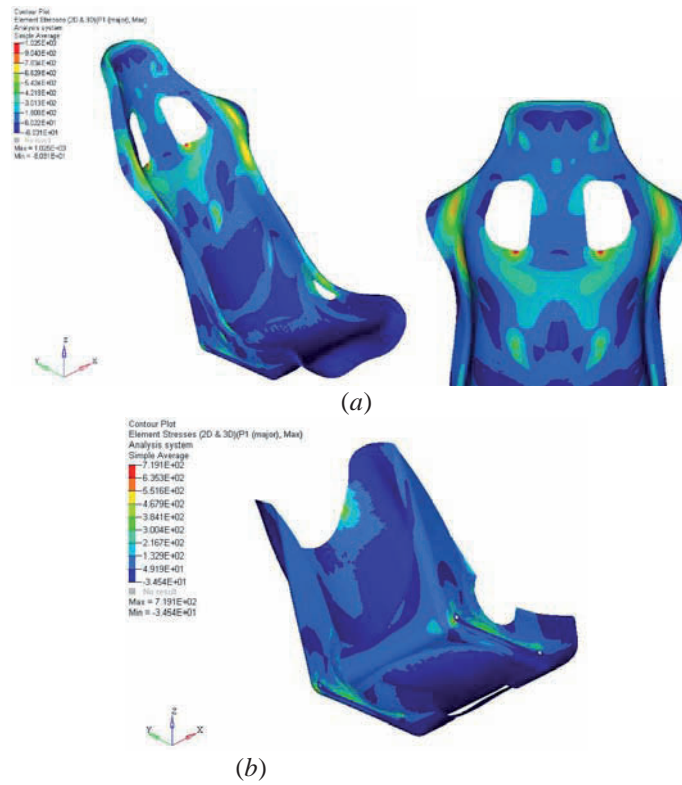


Figure 7: Design 2: Maximum principal stress distribution (a) of the seat and (b) of the lower shell.

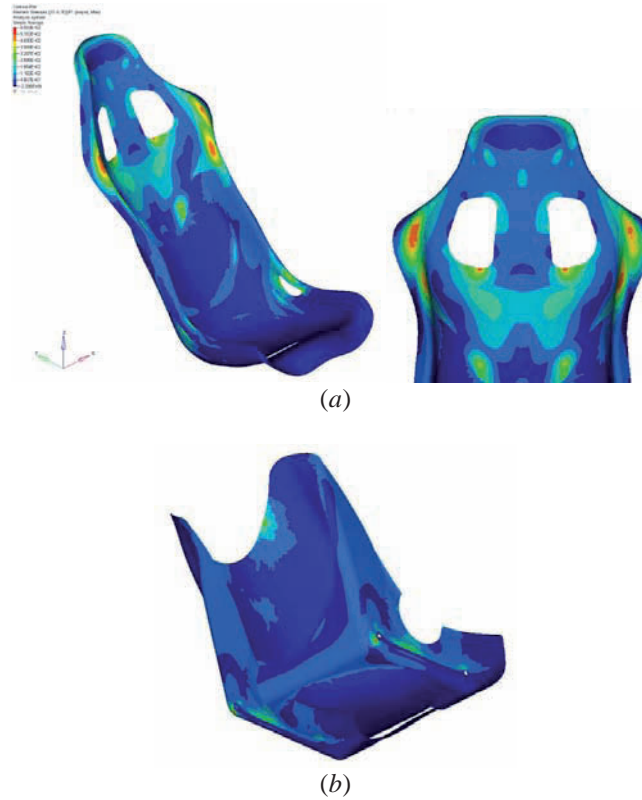


Figure 8: Design 3: Maximum principal stress distribution (a) of the seat and (b) of the lower shell.

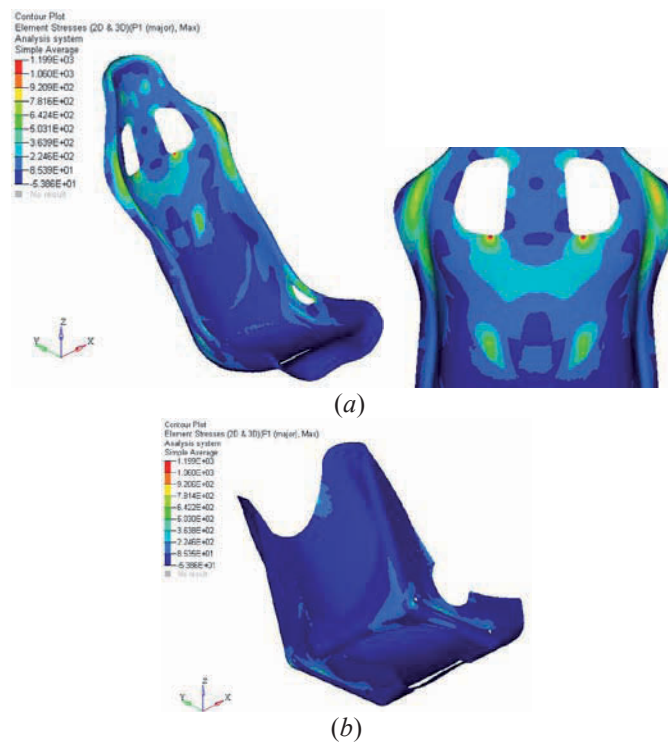


Figure 9: Design 4: Maximum principal stress distribution (a) of the seat and (b) of the lower shell.



Figure 10: Design 1: Failure index corresponding to the Tsai-Hill anisotropic criterion for the seat and its lower shell.



Figure 11: Design 2: Failure index corresponding to the Tsai-Hill anisotropic criterion for the seat and its lower shell.



Figure 12: Design 3: Failure index corresponding to the Tsai-Hill anisotropic criterion for the seat and its lower shell.

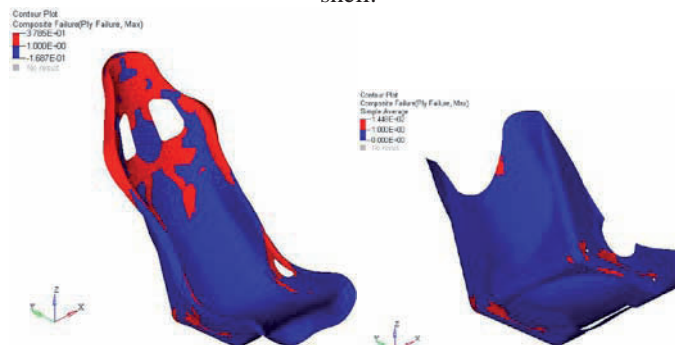


Figure 13: Design 4: Failure index corresponding to the Tsai-Hill anisotropic criterion for the seat and its lower shell.

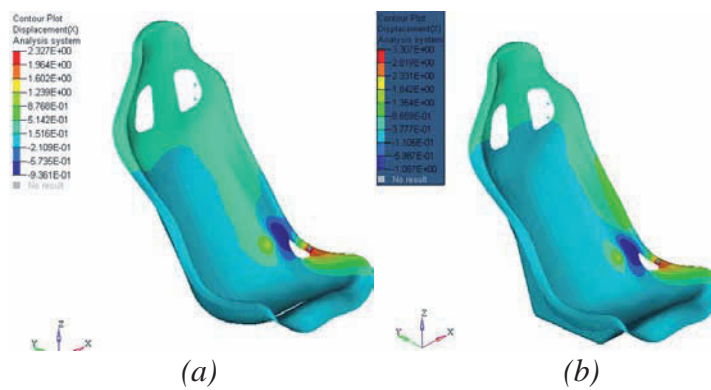


Figure 14: Displacements in the direction x (side) for: (a) Design 1 and (b) Design 4.

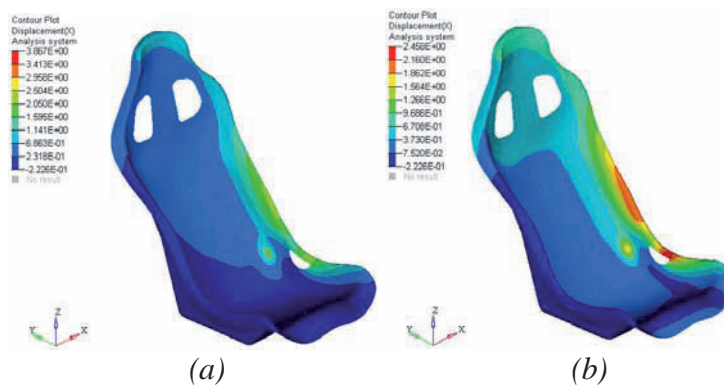


Figure 15: Displacements in the direction x (side) for: (a) Design 3 and (b) Design 4.

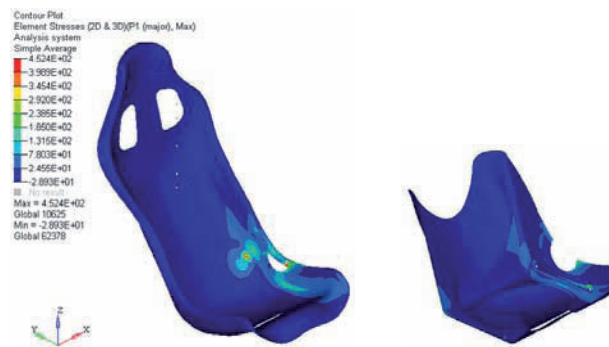


Figure 16: Design 1: Distribution of the maximum principal stress on the seat and lower shell.

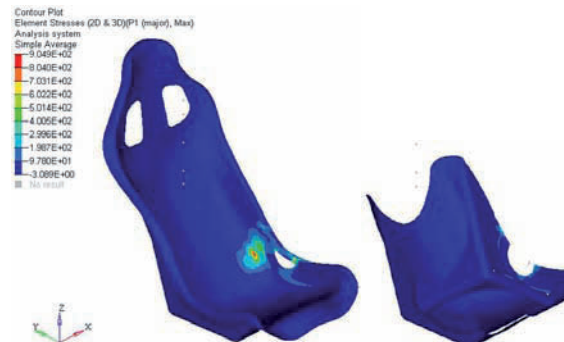


Figure 17: Design 2: Distribution of the maximum principal stress on the seat and lower shell.



Figure 18: Design 3: Distribution of the maximum principal stress on the seat and lower shell.



Figure 19: Design 4: Distribution of the maximum principal stress on the seat and lower shell.

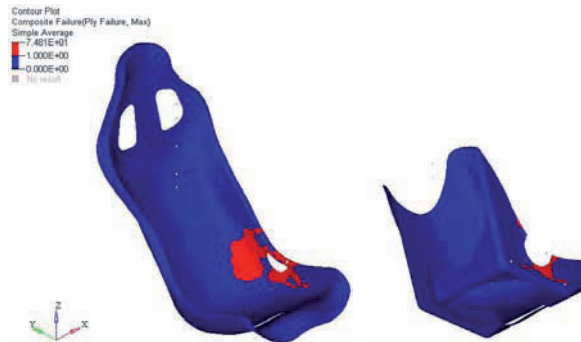


Figure 20: Design 1: Failure index corresponding to the Tsai-Hill criterion on the seat and lower shell.

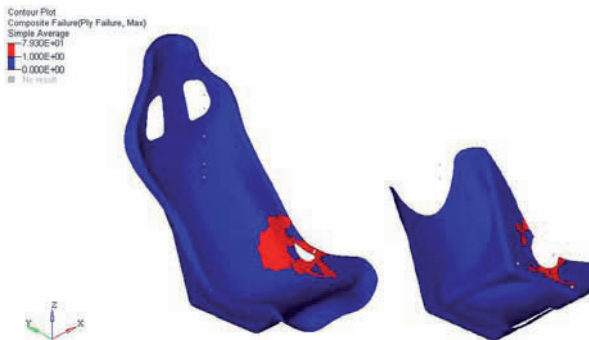


Figure 21: Design 2: Failure index corresponding to the Tsai-Hill criterion on the seat and lower shell.

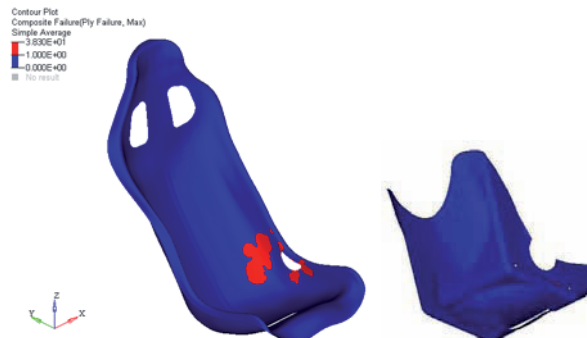


Figure 22: Design 3: Failure index corresponding to the Tsai-Hill criterion on the seat and lower shell.



Figure 23: Design 4: Failure index corresponding to the Tsai-Hill criterion on the seat and lower shell.

4 CONCLUDING REMARKS

Following the specification given on Standard 8862, two quasi-static numerical tests (one rear and one side) have been performed for a composite seat.

Four lay-ups of the composite material have been considered for the simulations: Design 1 considers one woven carbon/resin, seven tri-axial glass/resin layers for the seat, and seven tri-axial glass/resin layers for the lower shell; Design 2 considers one woven carbon/resin, five tri-axial glass/resin layers for the seat, and five tri-axial glass/resin layers for the lower shell; Design 3 considers seven tri-axial glass/resin layers for the seat, and seven tri-axial glass/resin layers for the lower shell; Design 4 considers one woven carbon/resin, eight bidiagonal carbon/resin layers for the seat, and five tri-axial glass/resin layers for the lower shell.

Assuming a purely elastic behaviour of the composite material, i.e. of the carbon fibre and also of the glass fibre layers, the total displacement distribution has been computed which, for Design 1 and Design 4, remains within the specified limits for the rear and side tests. Concentration of high stresses in correspondence of the loading pads, the shoulder edges, and the belt's slots appear to fail. Moreover, the woven carbon fibre layer appears completely damaged, when combined with the tri-axial glass fibre layers, and with localized damage when combined with bi-directional carbon fibre layers.

Regarding the lower shell part of the seat, critical values of stresses and consequently failure appearance has been found around the attachment points.

REFERENCES

- Federation Internationale De L'automobile, Norme 8855-1999, Standard 8855-1999, Norme FIA Pour Sieges De Competition, FIA Standard For Competition Seats, 2003.
- Federation Internationale De L'automobile, Norme 8862-2009, Standard 8862-2009, Siege De Competition Haute, Performance Advanced Racing Seat, 2010.
- ALTAIR, www.altair.com, 2010.
- SAERTEX, www.saertex.com, 2010.